JOURNAL OF APPLIED ELECTROCHEMISTRY **28** (1998) 993–998

Differential capacitance studies of the specific adsorption of thiosulfate on silver

R. SRINIVASAN, I. I. SUNI

Department of Chemical Engineering, Clarkson University, Potsdam, NY 13699-5705, USA

Received 3 June 1997; revised 7 January 1998

The differential capacitance of a polycrystalline Ag electrode was measured in a $NaClO_4$ electrolyte containing $Na_2S_2O_3$ at concentrations ranging from 0.1 to 20 mM and at electrode potentials ranging from −0.9 to −0.3 V vs SCE. The differential capacitance measurements were analysed to obtain the surface coverage of specifically adsorbed thiosulfate ($S_2O_3^{2-}$) as a function of both electrode potential and bulk concentration. The various forms for the adsorption isotherm at an electrochemical interface which are commonly employed are reviewed and discussed. The adsorption behaviour is best explained by the formation of image dipoles by the specifically adsorbed ions, whose energetic interactions are then dominated by repulsion of like dipoles. The adsorption data is quantitatively fit to an adsorption isotherm for interacting dipoles, yielding an effective dipole moment of 0.72 *D* for the system $S_2O_3^{2-}$/Ag.

Keywords: *thiosulfate*, *silver*, *adsorption*, *differential capacitance*

List of symbols

C_d	differential capacitance
C_H	Helmholtz capacitance
c	bulk concentration of $Na_2S_2O_3^{2-}$
E	electrode potential
e	electronic charge
ΔG^0_{ads}	standard Gibbs free energy of adsorption
g_0	parameter in the Frumkin adsorption isotherm characterizing strength of interactions
g_1	parameter characterizing strength of interactions for adsorbed layer of charges
g_2	parameter characterizing strength of interactions for adsorbed layer of dipoles
k	exponent defining a constant phase element (c.p.e.)
m	two-dimensional surface coordination number
n	number of sites involved in multisite adsorption
Q	constant related to impedance
q	excess electronic charge density at electrode surface
R	universal gas constant
R_s	solution resistance
r	nearest neighbour distance at full coverage
T	temperature
x	mol fraction of $Na_2S_2O_3^{2-}$
Z	impedance
z	ionic charge in unsigned units of electronic charge

Greek symbols

γ	surface tension
γ'	electrosorption valency
Γ_s	surface excess of $S_2O_3^{2-}$
Γ_c	surface excess of ClO_4^-
Γ'_s	specifically adsorbed concentration of $S_2O_3^{2-}$
Γ'_c	specifically adsorbed concentration of ClO_4^-
θ	fractional surface coverage
κ, κ'	constants which appear in adsorption isotherms
μ	dipole moment
ω	angular frequency of oscillation

1. Introduction

Thiosulfate ($S_2O_3^{2-}$) is widely employed industrially as a Ag^+ complexing agent during image development in photography [1]. Through reduction of the Ag^+ activity in solution, thiosulfate promotes fixing of photographic films by selective dissolution of AgX while leaving neutral Ag intact [2]. Although other species may solvate Ag^+ ions, none has a better combination of solvation ability, cost, nontoxicity, and stability during dilution by washing. Thiosulfate also has potential applications in development of noncyanide silver plating baths. This has motivated a series of recent studies by Vereecken and coworkers to elucidate the thermodynamic and kinetic aspects of silver oxidation/reduction from thiosulfate complexes [3–8].

However, little is known of the adsorption of thiosulfate on Ag. Early studies of silver image fixation showed that thiosulfate adsorbed strongly on silver surfaces immersed in thiosulfate-containing solutions [9, 10]. Although thiosulfate was initially believed to adsorb in the form of AgS, the inability to remove this deposit with a cyanide solution led to the

0021-891X

suggestion that thiosulfate forms a single atomic layer of S, similar to the phenomenon of underpotential deposition, rather than forming discrete AgS [10]. More recently, detection of thiosulfate adsorption has been reported by differential capacitance [11, 12], although these investigators reported that their adsorption measurements were only qualitative due to reaction of thiosulfate with the silver surface. In addition, recent surface-enhanced Raman spectroscopy (SERS) investigations found evidence for a surprising phenomenon, an increase in the extent of thiosulfate adsorption on silver with increasing bulk concentration of nitrate ion [8]. This paper reports differential capacitance measurements of thiosulfate adsorption on Ag electrodes at a variety of bulk concentrations and demonstrates that the appropriate adsorption isotherm is that for an array of repulsively interacting image dipoles.

2. Experimental details

All reagents were prepared with water that was purified by deionization, reverse osmosis, and filtration and then by double distillation. Cleanliness was ensured by observing both cyclic voltammagrams and differential capacitance as a function of time for an electrolyte solution containing a nonadsorbing anion, ClO_4^-. These experiments indicated that the surface remained effectively uncontaminated for approximately 1–2 h. Electrochemical measurements were conducted in a Pyrex cell using a Pt spiral counter electrode and a SCE reference electrode with an EG&G model 263A potentiostat. All potentials are reported with respect to SCE. The 7 mm diameter >99.99% polycrystalline Ag working electrode (Aldrich) was embedded in a Teflon mount and affixed with TorrSeal, a highly chemically inert epoxy. Prior to each experiment, the electrode and mount were mechanically polished with successively finer grades of alumina down to 0.05 μm in diameter, followed by rinsing and sonication in ultrapure water to remove any attached alumina particles. During immersion into the electrochemical cell, the electrode was potentiostated, and, following immersion, the cell potential was cycled several times. This pretreatment was sufficient to yield differential capacitance curves congruent to those obtained by previous investigators for a blank $NaClO_4$ electrolyte [13]. All solutions were deoxygenated by bubbling Ar through the electrolyte for approximately 20 min. The pH was approximately 5.8 for all solutions employed.

Capacitance was measured by phase sensitive detection using a Stanford Research Systems model SR830 lock-in amplifier by measuring the current component which lags the applied AC voltage by 135° [14]. An AC voltage of 2 mV was applied at a frequency of 50 Hz, where the capacitance measurements were approximately independent of frequency. Potential sweeps at 2 mV s^{-1} were employed to determine the potential dependence of the capacitance, yielding capacitance values that depended on the sweep direction by less than 3%.

3. Results

A typical cyclic voltammogram for 10 mM $Na_2S_2O_3$/Ag is shown in Fig. 1. Oxidation starts at approximately −0.25 V, reflecting the strong interaction of thiosulphate ions with Ag surfaces. Since even small faradaic currents can alter the phase relationship between the current and voltage, differential capacitance measurements were only recorded at potentials cathodic of −0.3 V. Differential capacitance measurements performed at sweep rates of 2 mV s^{-1} are shown in Fig. 2 for several different bulk thiosulfate

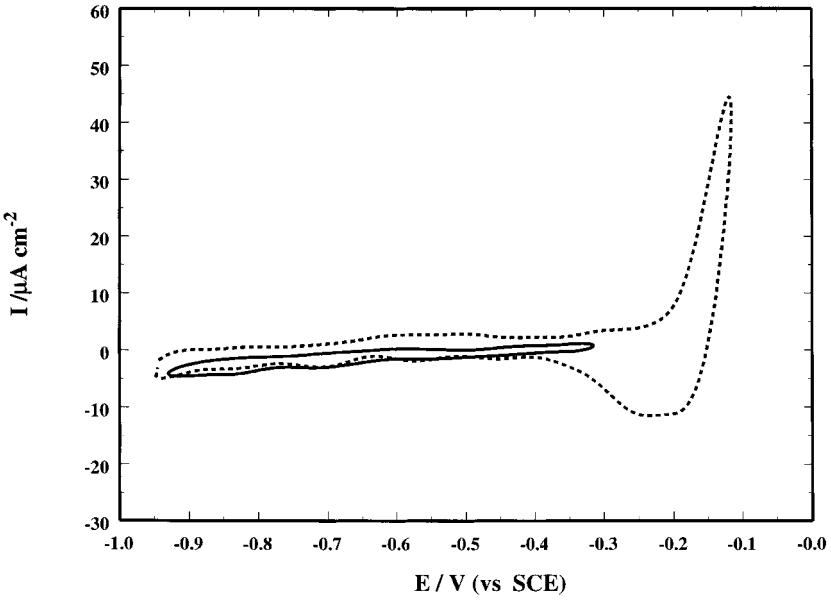

Fig. 1. Cyclic voltammogram for 10 mM $Na_2S_2O_3$, 0.49 M $NaClO_4$ solution at a sweep rate of 5 mV s^{-1}. Dashed curve: voltammogram on a Ag surface roughened by oxidation-reduction cycling. Solid curve: voltammogram on an unroughened Ag surface.

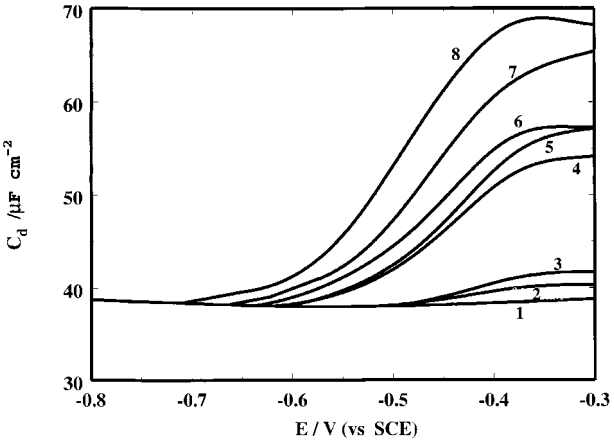

Fig. 2. Differential capacitance measurements for a mixed electrolyte of $NaClO_4$ and various $Na_2S_2O_3$ concentrations at a total ionic strength 0.5 M and a sweep rate of 2 mV s^{-1}. The $Na_2S_2O_3$ concentrations are 0 (1), 0.1 (2), 0.2 (3), 1.0 (4), 1.5 (5), 2.0 (6), 10 (7) and 20 mM (8).

concentrations with the total ionic strength constant at 0.5 M. These measurements were reproducible over repeated voltage sweeps, demonstrating that adsorption was reversible and that the surface roughness did not increase significantly. This and other internal consistency checks also demonstrate that no significant faradaic currents are present at potentials below −0.3 V. Thiosulfate adsorption appeared to approach saturation above bulk concentrations of about 30–50 mM, as evidenced by the saturation of the differential capacitance curves.

Differential capacitance measurements were analysed as described by Weaver and coworkers [13] for conditions where the total ionic strength is kept constant while varying the molar fraction x of the specifically adsorbing anion, in this case $S_2O_3^{2-}$. The surface excess of $S_2O_3^{2-}$ was determined using a Hurwitz–Parsons analysis, where for a mixed electrolyte with only one adsorbing anion, the Gibbs adsorption isotherm can be written as [15]

$$-\mathrm{d}\gamma = q\,\mathrm{d}E + \left[\Gamma_s - \left(\frac{x}{0.5-x}\right)\Gamma_c\right] RT\,\mathrm{d}\,\ln x \qquad (1)$$

where the symbols are as listed at the outset. As long as neither anion preferentially populates the diffuse layer, one can rewrite Equation 1 as [13]

$$-\mathrm{d}\gamma = q\,\mathrm{d}E + \left[\Gamma'_s - \frac{x}{0.5-x}\Gamma'_c\right] RT\,\mathrm{d}\,\ln x \qquad (2)$$

where Γ'_s and Γ'_c are the specifically adsorbed concentrations of the two anions. The second term above in parentheses is assumed to be negligibly small. In this case Γ'_s can be obtained by differentiating the surface tension in Equation 2 with respect to the mole fraction x:

$$\Gamma'_S = -\frac{1}{RT}\left(\frac{\partial\gamma}{\partial \ln x}\right)_E \qquad (3)$$

The surface tension at each mole fraction x was obtained by doubly integrating the experimental curves of differential capacitance, with integration beginning at −0.95 V. The derivative in Equation 3 was obtained by graphical differentiation of plots of the surface tension γ against $\ln x$ at each electrode potential E [16]. Figure 3 shows the surface concentration obtained from Equation 3 as a function of electrode potential and bulk concentration of thiosulfate. The roughness factor during the present experiments was found to be approximately 1.31 from measurements of Pb underpotential deposition.

Several potential complications to the differential capacitance measurements reported here deserve comment. Both Hg and solid electrodes can exhibit nonideal interfacial capacitance behaviour for a variety of reasons, so the interfacial impedance is often represented by a constant phase element (c.p.e.) [17]

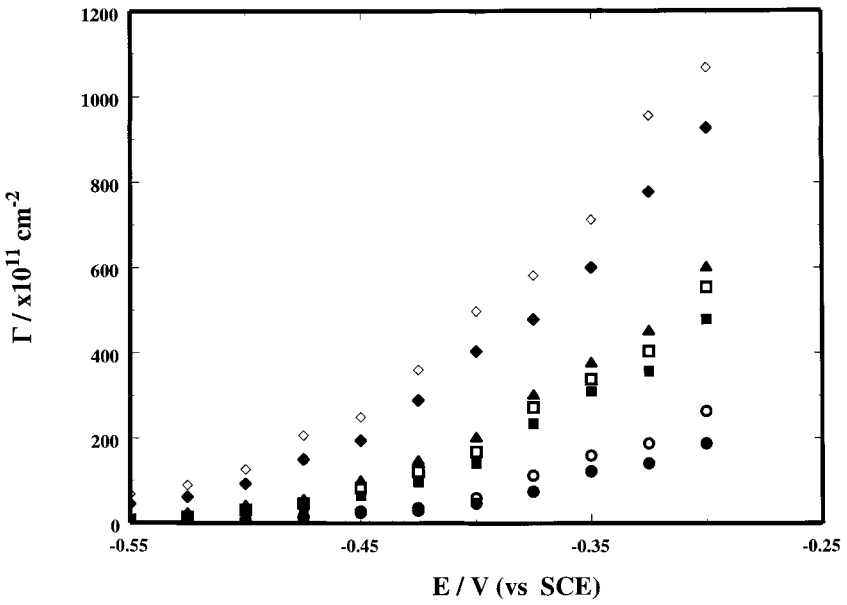

Fig. 3. Surface coverage of $S_2O_3^{2-}$ as a function of potential. Key: (●) 0.1, (○) 0.2, (■) 1.0, (□) 1.5, (▲) 2.0, (◆) 10.0 and (◇) 20.0 mM. The surface coverages have been adjusted to reflect a roughness factor of 1.31.

$$Z(\omega) = R_s + Q(i\omega)^{-k} \quad (4)$$

The symbols are specified at the outset. For a purely capacative interfacial impedance, k is equal to one. However, such a treatment makes determination of an adsorption isotherm problematic, since the constant Q cannot be associated with a capacitance when k is not equal to one. Indeed, this is a general problem that makes adsorption isotherms quite difficult to measure by impedance spectroscopy, since equivalent circuit elements cannot be easily associated with the interfacial capacitance.

For solid electrodes, some authors have associated the observation of a c.p.e. with the presence of surface roughness, which reflects heterogeneity of surface sites with different energetics. However, a number of authors have questioned the idea of a simple connection between a c.p.e. and surface roughness [18–20], so this association remains controversial. Nonideality in the solution phase is also believed to yield a c.p.e. [21, 22], the origin of which has been ascribed to problems with the solution conductivity. In summary, although the experimental observation of a c.p.e. is established for a number of systems, its origins have proven difficulty to identify and quantify and thus remain controversial [23, 24]. However, one can get an approximate idea of the degree of impedance nonideality by comparison to results reported for polycrystalline pt electrodes in perchloric acid solutions [23]. In this case solution-phase nonidealities were not present at an ionic strength of 0.5 M, an unsurprising result given the limited spatial extent of the diffuse layer at these concentrations. In addition, k was found to be very close to unity for the low roughness values (1.31) seen in the current study. Differential capacitance can be problematic for the reasons given here and others. Indeed, few cases may exist where it is absolutely rigorous. However, this technique has been applied most extensively to and is well-established on Ag electrodes [13, 25–29].

Recent surface-enhanced Raman spectroscopy (SERS) investigations have suggested that the extent of thiosulfate adsorption on silver increases with increasing bulk concentration of nitrate ion [8]. This is consistent with the observation that the integrated intensity under an unassigned SERS $S_2O_3^{2-}$ peak, which appears at concentrations below the bulk detection limit, increases by a factor of 2–3 × in the presence of 0.5–0.6 M $NaNO_3$. Evidence for such cooperative behaviour was sought by comparing the differential capacitance curve against electrode potential for an electrolyte containing 10 mM $NaNO_3$, 10 mM $Na_2S_2O_3$ and 0.48 M $NaClO_4$ to the curve reported in Fig. 2 for 10 mM NaS_2O_3 and 0.49 M $NaClO_4$. These two curves were virtually identical, suggesting the cooperative effects of $NaNO_3$ on $S_2O_3^{2-}$ adsorption are insignificant at low concentrations of $NaNO_3$. This is a legitimate comparison because several control experiments showed that the differential capacitance of a blank 0.5 M $NaClO_4$ electrolyte differed insignificantly from that for 10 mM $NaNO_3$ and 0.49 M $NaClO_4$. This comparison is difficult at $NaNO_3$ concentrations as high as those employed by previous investigators [8] due to strong effects of the background anion on the baseline capacitance.

4. Discussion

The ability to relate surface coverage at the solid–liquid interface to bulk concentration, that is the determination of the adsorption isotherm, can be of significant practical importance in understanding the behaviour of plating additives, of surfactants, and of surface processes in biomedical technology. Adsorption isotherms in electrochemical systems have been reviewed by Conway [30] and will be summarized only briefly. The familiar Langmuir adsorption isotherm arises from considering site competition but neglecting both interactions between adsorbed species and surface heterogeneity. The Langmuir isotherm relates surface coverage (θ) to bulk concentration c according to

$$\frac{\theta}{1-\theta} = \kappa c \quad (5)$$

On the other hand, noninteracting species which occupy multiple (n) adsorption sites may follow what will be called the multisite adsorption isotherm [31]:

$$\frac{\theta}{(1-\theta)^n}\frac{[\theta + n(1-\theta)]^{n-1}}{n} = \kappa c \quad (6)$$

The Temkin isotherm may be applicable to adsorption of uncharged, noninteracting species onto a heterogeneous surface, where the adsorption energy varies with adsorption site [32, 33]. The Temkin isotherm is usually written as:

$$\theta = \kappa \log c \quad (7)$$

Interactions between adsorbed species can be included in a variety of different ways, but are most commonly ascribed to a Frumkin isotherm, which can be written as:

$$\frac{\theta}{1-\theta} = \kappa c\, e^{-g_0\theta} \quad (8)$$

This form can be derived, for example, assuming pairwise nearest-neighbour interactions [30]. The parameter g_0 characterizes the strength of the two-dimensional interactions in the adlayer and is sometimes found to be potential dependent. The Frumkin isotherm reduces mathematically to the Temkin isotherm for cases of strong adsorption.

Although the Frumkin isotherm is widely employed, it lacks a direct theoretical connection to a realistic form for the adlayer interaction energy. If one considers the present case of adsorption of ionic species, an adsorption isotherm can be derived for a coverage-dependent coulombic interaction energy of the form $g_1 RT\theta^{1/2}$, yielding [30]

$$\frac{\theta}{1-\theta} = \kappa c\, e^{-g_1\theta^{-1/2}} \tag{9}$$

This isotherm will be referred to as the charge isotherm. Here it is expected that

$$g_1 = \frac{mz^2}{2RTr} \tag{10}$$

where m, R, T, z, and r are as listed at the outset. More realistically, one might expect ionic adsorption to create an image charge in the electrode, forming an image dipole. In this case the adsorption isotherm can be derived from the coverage-dependent interaction energy of the form $g_1RT\theta^{3/2}$, yielding [34]

$$\frac{\theta}{1-\theta} = \kappa c\, e^{-3g_2\theta^{1/2}} \tag{11}$$

This will be referred to as the dipole isotherm. Here, neglecting the consideration of partial charge transfer and the electrosorption valency,

$$g_2 = \frac{m\mu^2}{2RTr^3} \tag{12}$$

where μ is the dipole moment. Each of the above constants κ are in reality the product of other constants according to

$$\kappa = \kappa' e^{-\Delta G^0_{ads}/RT} e^{VF/RT} \tag{13}$$

where ΔG^0_{ads} is the Gibbs free energy of adsorption. The second exponential term arises from the equilibrium condition that the bulk chemical potential be equal to that at the electrochemical interface, which is exponentially related to the electrode potential. Unfortunately, ΔG^0_{ads} can vary with potential, making separation of the different components of Equation 13 difficult.

Independent numerical least-squares fits of the surface coverage (θ) to the bulk concentration c at ten different electrode potentials were performed to test the applicability of the above adsorption isotherms. The Langmuir, multisite and charge isotherms provided poor fits and will not be considered further. The Temkin isotherm was rejected on the basis of the consistent deviations in the same direction found at each of the ten potentials examined. This could be visually observed from plots with θ as the ordinate and log c as the abcissa that were all slightly concave upward rather than linear. Both the Frumkin and dipole isotherms provided fits that were reasonably appealing to the naked eye. However, the Frumkin isotherm was rejected for two reasons. First, the total residual variance over the ten data sets was approximately 55% lower for the dipole isotherm relative to the Frumkin isotherm. In addition, if one allowed ten different values for g_2 in the dipole isotherm, these agreed to within approximately 25%, whereas the ten different values for g_0 varied by as much as 70% from their average value.

Thus the dipole isotherm given by Equation 11 provides a superior data fit with effectively fewer adjustable parameters. In addition, this isotherm is consistent with a simple and intuitively reasonable model for the adlayer interactions of specifically adsorbed anions. A plausible model is that adsorbed species form image dipoles, with the adlayer energetics dominated to first order by repulsive dipole interactions. To the author's knowledge this is the first time that the dipole isotherm has been verified as the best description for the specific adsorption of a particular ionic species. The dipole isotherm may not describe specific adsorption of all ionic species due to partial charge transfer, dipole depolarization, ion pairing effects, and other nonideal behaviour. The least-squares fit of the experimental data to the dipole

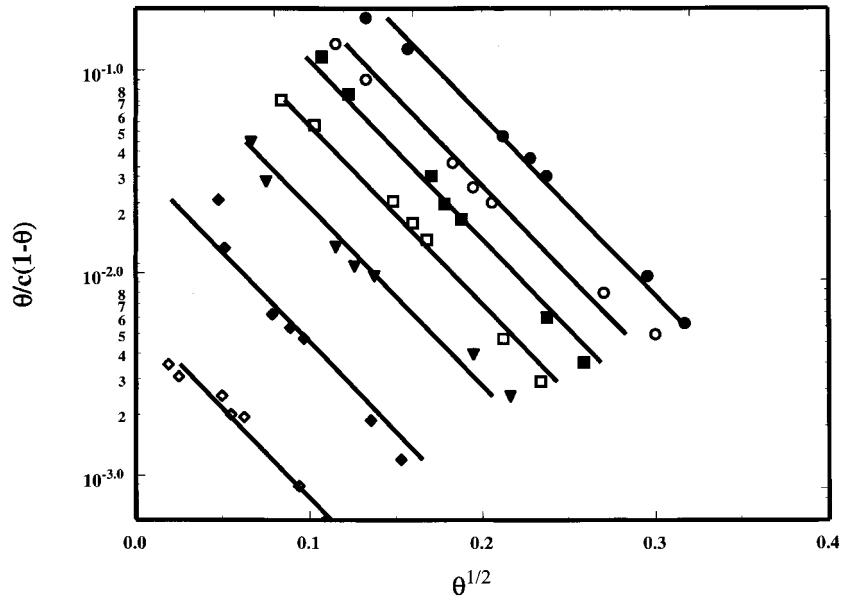

Fig. 4. Comparison of the experimental data to the adsorption isotherm for repulsive, parallel image dipoles. Key: (●) −0.30, (○) −0.325, (■) −0.35, (□) −0.375, (▲) −0.40, (◆) −0.45, and (◇) −0.50 V.

Table 1. Variation of κ with electrode potential

Potential/V vs SCE	ln κ
−0.300	1.24
−0.325	0.45
−0.350	−0.16
−0.375	−0.90
−0.400	−1.83
−0.425	−2.64
−0.450	−3.36
−0.475	−4.24
−0.500	−5.13
−0.525	−6.03

isotherm is shown in Fig. 4. Table 1 gives the potential-dependent best-fit values for κ, and the best fit value for g_2 is approximately 6.8. From Equation 12, assuming a coordination number of six and that r is the nearest-neighbour spacing on Ag(111), a dipole moment of 0.72 D is obtained for the $S_2O_3^{2-}$/Ag system. This value can be compared to that predicted by approximating the dipole moment as [35]

$$\mu = \frac{ze}{4\pi C_H}\left(1 - \frac{\gamma'}{z}\right) \tag{14}$$

where C_H is the Helmholtz double-layer capacitance and z times the quantity in parentheses is the effective number of charges in the adsorbed species. The extraction of the Helmholtz capacitance from differential capacitance measurements is difficult [36, 37], so an approximate value of 70 μF cm^{-2} has been taken, yielding a dipole moment of 1.2 D. This is of the same magnitude as that measured,which is probably reduced in size by the nonideal behaviour mentioned above. The noise in the differential capacitance measurements mask any variation in the dipole moment with potential, so only an average value is reported.

5. Conclusions

A combination of cyclic voltammetry and differential capacitance measurements show that $S_2O_3^{2-}$ specifically adsorbs on a polycrystalline Ag electrode in measurable quantities between approximately −0.7 V and −0.3 V vs SCE, at which point the adsorbed species undergoes faradaic reaction. The surface coverage as a function of bulk concentration and electrode potential has been determined and shown to be consistent with an isotherm previously proposed for the interaction of parallel image dipoles according to [34]

$$\frac{\theta}{1-\theta} = \kappa c\, e^{-3g_2\theta^{1/2}} \tag{15}$$

where

$$g_2 = \frac{m\mu^2}{2RTr^3} \tag{16}$$

Numerical fits to this isotherm yield an effective dipole moment of 0.72 D, which is roughly consistent with that expected from a simple model of the electrochemical interface.

Acknowledgement

This research was supported by NSF grant CTS-9527497.

References

[1] See for example, 'The Theory of Photographic Processes' (edited by T.H. James), MacMillan, New York (1977).
[2] G. I. P. Levenson, *in* [1], pp. 437–61.
[3] S. Vandeputte, B. Tribollet, A. Hubin and J. Vereecken, *Electrochim. Acta* **39** (1994) 2729.
[4] A. Hubin and J. Vereecken, *J. Appl. Electrochem.* **24** (1994) 239.
[5] *Idem*, *ibid.* **24** (1994) 396.
[6] S. Vandeputte, E. Verboom, A. Hubin and J. Vereecken, *J. Electroanal. Chem.* **397** (1995) 249.
[7] B. van den Bossche, L. Bortels, J. Decominck, S. Vandeputte and A. Hubin, *ibid.* **397** (1995) 35.
[8] D. Gonnissen, S. Vandeputte, A. Hubin and J. Vereecken, *Electrochim. Acta* **41** (1996) 1051.
[9] G. W. W. Stevens and P. Block, *J. Photogr. Sci.* **7** (1959) 111.
[10] P. A. Block and G. W. W. Stevens, *ibid.* **9** (1961) 330.
[11] T. Ramstad and M. J. Weaver, *J. Chromatogr.* **456** (1988) 307.
[12] T. Ramstad and D. Milner, *Anal. Instrum.* **18** (1989) 147.
[13] J. T. Hupp, D. Larkin and M. J. Weaver, *Surf. Sci.* **125** (1983) 429.
[14] A. J. Bard and L. R. Faulkner, 'Electrochemical Methods', J. Wiley & Sons, New York (1980).
[15] E. Dutkkiewicz and R. Parsons, *J. Electroanal. Chem.* **11** (1966) 100.
[16] H. S. Fogler, 'Elements of Chemical Reaction Engineering', 2nd edn. Prentice Hall, Englewood Cliffs, NJ (1992).
[17] G. J. Brug, A. L. G. van den Eeden, M. Sluyters-Rehbach and J. H. Sluyters, *Electrochim. Acta* **176** (1984) 275.
[18] A. L. G. van den Eeden, 'Metal Structure and Double Layer Capacity', PhD thesis, University of Utrech, The Netherlands (1984).
[19] J. B. Bates, Y. T. Chu and W. T. Stribling, *Phys. Rev. Lett.* **60** (1988) 627.
[20] T. Pajkossy, *J. Electroanal. Chem.* **364** (1994) 111.
[21] P. H. Bottelberghs and G. H. J. Broers, *ibid.* **67** (1976) 155.
[22] W. Scheider, *J. Phys. Chem.* **79** (1975) 127.
[23] E. D. Bidoia, L. O. S. Bulhoes and R. C. Rocha-Filho, *Electrochim. Acta* **39** (1994) 763 and references therein.
[24] G. Lang and K. E. Heusler, *J. Electroanal. Chem.* **391** (1995) 169 and references therein.
[25] G. Valette, A. Hamelin and R. Parsons, *Z. Phys. Chem. N.F.* **113** (1978) 71.
[26] D. Larkin, K. L. Guyer, J. T. Hupp and M. J. Weaver, *Surf. Sci.* **138** (1982) 401.
[27] M. J. Weaver, F. Barz, J. G. Gordon II and M. R. Philpott, *ibid.* **125** (1983) 409.
[28] M. J. Weaver, J. T. Hupp, F. Barz, J. G. Gordon II and M. R. Philpott, *ibid.* **160** (1984) 321.
[29] M. Bacchetta, S. Trasatti, L. Donbova and A. Hamelin, *J. Electroanal. Chem.* **255** (1988) 237.
[30] B. E. Conway, *Prog. Surf. Sci.* **16** (1984) 1.
[31] J. O'M. Bockris, *J. Electrochem. Soc.* **111** (1964) 736.
[32] D. O. Hayward and B. M. Trapnell, 'Chemisorption', 2nd edn, Butterworths, London (1964), chapter 5.
[33] D. M. Young and A. D. Crowell, 'Physical Adsorption of Gases', Butterworths, London (1962), chapter 7.
[34] B. E. Conway and H. Angerstein-Kozlowska, *J. Electroanal. Chem.* **113** (1980) 63.
[35] W. Schmickler, *ibid.* **249** (1988) 25.
[36] E. Panzram, H. Baumgartel, B. Roelfs, C. Schroter and T. Solomun, *Ber. Bunsenges. Phys. Chem.* **99** (1995) 827.
[37] A. Hamelin, Z. Borkowska and J. Stafiej, *J. Electroanal. Chem.* **189** (1985) 85.